Inorganica Chimica Acta, 198-200 (1992) 211-217

The 1,3-dimetalloallyl tri-ruthenium cluster $(\mu\text{-H})Ru_3(\mu_3\text{-}\eta^3\text{-CHCHCMe})(CO)_9$ and its PPh_3 derivatives

K. Mohan Rao, Robert J. Angelici*

Ames Laboratory and Department of Chemistry, Iowa State University, Ames, IA 50011 (USA)

and Victor G. Young, Jr.

Iowa State University Molecular Structure Laboratory, Iowa State University, Ames, IA 50011 (USA)

Abstract

Reactions of $Ru_3(CO)_{12}$ with 1,3-butadiene or *cis*-2-butene give the $\mu_3\text{-}\eta^3$-dimetalloallyl compound $(\mu\text{-H})Ru_3(\mu_3\text{-}\eta^3\text{-CHCHCMe})(CO)_9$ (**2**). Refluxing **2** with PPh_3 gives the CO-substituted products $(\mu\text{-H})Ru_3(\mu_3\text{-}\eta^3\text{-CHCHCMe})(CO)_8(PPh_3)$ (**3**) and $(\mu\text{-H})Ru_3(\mu_3\text{-}\eta^3\text{-CHCHCMe})(CO)_7(PPh_3)_2$ (**4**). Single crystal X-ray diffraction studies of **2**, **3** and **4** show that all have the dimetalloallyl unit. These investigations demonstrate that this unit is remarkably stable and might be expected to form on triangular arrays of metal atoms on metal surfaces.

Introduction

When ethylene is adsorbed on ruthenium metal supported on silica, weakly adsorbed ethane, *cis*- and *trans*-2-butene and butane are formed as ascertained by solid state ^{13}C NMR studies [1]. In addition, there are ^{13}C NMR peaks for chemisorbed species whose identities are not unequivocally established. In an effort to characterize such species by comparing their ^{13}C NMR spectra with those of trinuclear ruthenium complexes containing hydrocarbon ligands analogous to those which may form on the ruthenium surface, we have examined reactions of $Ru_3(CO)_{12}$ with ethylene, *cis*-2-butene and 1,3-butadiene. It is known [2] that $Ru_3(CO)_{12}$ reacts with ethylene to give a mixture of seven products among which was $(\mu\text{-H})Ru_3(\mu_3\text{-}\eta^3\text{-CEtCHCMe})(CO)_9$ (**1**). Although the yield was low in this reaction, other $(\mu\text{-H})Ru_3(\mu_3\text{-}\eta^3\text{-CR}^1\text{CR}^2\text{CR}^3)(CO)_9$ complexes have been prepared [3] in much higher yields from reactions of the μ_3-carbyne complex $(\mu\text{-H})_3Ru_3(\mu_3\text{-CR}^1)(CO)_9$ with $R^2C{\equiv}CR^3$ and from $Ru_3(CO)_{12}$ with alkenes, dienes and alkynes [4]. The product $(\mu\text{-H})Ru_3(\mu_3\text{-}\eta^3\text{-CHCHCMe})(CO)_9$ (**2**) of the reaction of $Ru_3(CO)_{12}$ with 1,3-butadiene exhibited an unusually low field ^1H NMR signal (δ 8.52 ppm) for the terminal allyl proton H(2), which raised a question about the correctness of the structural assignment [4b]. In the present study, we repeated the synthesis of **2** from $Ru_3(CO)_{12}$ and 1,3-butadiene. Complex **2** is also formed from reactions of $Ru_3(CO)_{12}$ with *cis*-2-butene and of $H_4Ru_4(CO)_{12}$ with 1,3-butadiene. In addition, we have examined the reaction of **2** with PPh_3 seeking rearrangement or partial displacement of the $\mu_3\text{-}\eta^3$-CHCHCMe ligand. The structures of **2**, the phosphine mono-substitution product **3**, and the phosphine di-substitution product **4** have been established by X-ray diffraction studies; all contain the $\mu_3\text{-}\eta^3$-CHCHCMe ligand (Scheme 1).

Experimental

The IR, ^1H and ^{13}C NMR and mass spectra were recorded on Digilab FTS-7, Nicolet-710 FT IR, Varian VXR-300, Kratos MS-50 and Finnigan 4000 spectrometers, respectively. Carbon and hydrogen analyses were carried out by Galbraith Laboratories, Inc. $H_4Ru_4(CO)_{12}$ was prepared by the literature method [5].

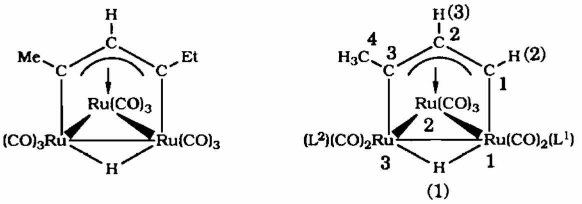

1

2: L^1 = CO, L^2 = CO
3: L^1 = CO, L^2 = PPh_3
4: L^1 = PPh_3, L^2 = PPh_3

Scheme 1.

---

*Author to whom correspondence should be addressed.

0020-1693/92/$5.00

Syntheses of $(\mu\text{-}H)Ru_3(\mu_3\text{-}\eta^3\text{-}CHCHCMe)(CO)_9$ (2)

Into a glass pressure vessel, $Ru_3(CO)_{12}$ (50 mg, 0.078 mmol) and dry degassed hexanes (30 ml) were placed. The vessel was pressurized with butadiene or *cis*-2-butene (20 to 30 psi) and then heated to 90 °C and stirred for 24 h. The resulting lemon–yellow solution was filtered and concentrated to 3–5 ml under vacuum. Unreacted $Ru_3(CO)_{12}$ was removed by filtration, and the filtrate was chromatographed on a silica gel column (1×20 cm) with hexanes. The eluent was concentrated and upon cooling to −25 °C gave orange crystals of **2** (yield: 24 mg, 50% from butadiene; 11 mg, 23% from cis-2-butene). *Anal.* Calc. for $C_{13}H_6O_9Ru_3$: C, 25.62; H, 0.99. Found: C, 25.62; H, 1.01%. IR ν(CO) cm^{-1} (hexane): 2097m, 2071s, 2045vs, 2027s, 2018m, 2010s, 1997w, 1959w. ^1H NMR (δ, ppm; $CDCl_3$): 8.52 d(H(2), 1H), 6.96 dd (H(3), 1H), 2.82s (Me, 3H), −20.41 d (H(1), 1H) ($J_{2,3} = 6.8$ Hz; $J_{1,3} = 2.38$ Hz). ^{13}C NMR (δ, ppm; $CDCl_3$): 39.13 (Me), 117.53 (C(2)), 159.45 (C(1)), 190.42 (C(3)), 200.0, 197.5, 195.89, 191.97 and 191.91 for CO groups. EI-MS: *m/e* 610.6 (M^+).

Synthesis of 2 from $H_4Ru_4(CO)_{12}$

A solution of $H_4Ru_4(CO)_{12}$ (50 mg, 0.067 mmol) in hexanes was heated at 90 °C under butadiene pressure in the pressure vessel for 20 h. The resulting brownish-orange solution was concentrated to a few ml and passed through a silica gel column (1×20 cm). A lemon–yellow eluent was collected, concentrated to a few ml and kept at −20 °C to yield orange crystals (yield 20%) of **2**.

Reaction of 2 with PPh_3

A 20 ml hexanes solution containing 80 mg (0.13 mmol) of **2** and excess PPh_3 (50 mg, 0.19 mmol) were refluxed with magnetic stirring for 24 h in a 50 ml Schlenk flask. The reaction mixture was evaporated under vacuum to near dryness; the suspension was transferred to a silica gel column (2×10 cm) and chromatographed using mixtures of hexanes and CH_2Cl_2 as the eluents. Five bands separated. The first and second bands were eluted with hexanes; the third band was eluted with 1:6 CH_2Cl_2–hexanes. The first band was unreacted **2**. The second band was the mono-substituted phosphine complex $(\mu\text{-H})Ru_3(\mu_3\text{-}\eta^3\text{-CHCHCMe})(CO)_8(PPh_3)$ (**3**) (yield: 30 mg, 27%) and the third band was the disubstituted phosphine complex $(\mu\text{-H})Ru_3(\mu_3\text{-}\eta^3\text{-CHCHCMe})(CO)_7(PPh_3)_2$ (**4**) (yield: 18 mg, 15%); both **3** and **4** are yellow–orange in color. Very small amounts (<1%) of two additional compounds, red and yellow bands, eluted with 1:4 CH_2Cl_2–hexanes; they were not characterized.

$(\mu\text{-H})Ru_3(\eta^3\text{-CHCHCMe})(CO)_8(PPh_3)$ (**3**): *Anal.* Calc. for $C_{30}H_{21}O_8PRu_3$: C, 42.70; H, 2.51. Found: C, 43.01; H, 2.72%. IR ν(CO) cm^{-1} (hexanes): 2081s, 2041vs, 2025 vs, 2002m, 1987m, 1969w. ^1H NMR (δ, ppm, $CDCl_3$) (atom labelling is given in Scheme 1): 8.52 (d, H(2), 1H), 6.93 (dd, H(3), 1H), 2.18 (d, Me, 3H, J(HP) = 4.45 Hz), 6.9–7.4 (m, Ph), −19.70 (dd, H(1), 1H, J(HP) = 15.3 Hz); $J_{2,3} = 6.62$ Hz, $J_{1,3} = 2.35$ Hz). ^{13}C NMR (δ, ppm, $CDCl_3$): 37.72 (C, Me), 118.01 (d, C(2), J(CP) = 1.5 Hz), 158.42 (C(1)), 194.96 (d, C(3), J(CP) = 7.05 Hz), 128.33 (d, Ph_m, J(CP) = 10.58 Hz), 130.33 (d, Ph_p, J(CP) = 2.0 Hz), 133.12 (d, Ph_0, J(CP) = 11.88 Hz), 135.53 (d, Ph_i, J(CP) = 48.35 Hz); 190.17 (d, CO, J(CP) = 4.0 Hz), 192.14, 195.7, 197.0 (d, CO, J(CP) = 3.53 Hz), 199.24 (d, CO, J(CP) = 2.02 Hz), 199.35 and 201.83 (d, CO, J(CP) = 8.56 Hz) are CO groups. ^{31}P NMR (δ, ppm; $CDCl_3$): 60.26. EI-MS: *m/e* 843 (M^+).

$(\mu\text{-H})Ru_3(\mu_3\text{-}\eta^3\text{-CHCHCMe})(CO)_7(PPh_3)_2$ (**4**): *Anal.* Calc. for $C_{47}H_{36}O_7P_2Ru_3 \cdot C_6H_{14}$: C, 54.79; H, 4.16. Found: C, 54.50; H, 4.25%. IR ν(CO) cm^{-1} (hexanes): 2049s, 2013vs, 1980m, 1974m, 1953w. ^1H NMR (δ, ppm, CD_2Cl_2): 7.33–7.2 (m, Ph), 2.19 (d, Me, 3H, J(HP) = 4.48 Hz). In $CDCl_3$: 7.5–6.9 (broad, Ph), 2.13 (d, Me, 3H, J(HP) = 4.49 Hz), −18.5 (H(1), broad). ^{13}C NMR (δ, ppm, CD_2Cl_2): 37.95 (t, Me, J(CP) = 3.9 Hz), 119.26 (C(2)), 195.62 (t, C(3), J(CP) = 1.8 Hz), 128.49 (dd, Ph_m, J(CP) = 8.56 Hz), 130.4 (d, Ph_p, J(CP) = 2.5 Hz), 133.82 (d, Ph_0, J(CP) = 12.08 Hz), 190.0–204.0 for CO groups. ^{31}P NMR (δ, ppm, $CDCl_3$): 64.81 (d, P(1), J(PP) = 14.7 Hz), 60.37 (d, P(2), J(PP) = 16 Hz). FAB-MS in CH_2Cl_2-3-nitrobenzyl alcohol matrix *m/e* 1078.8 (M^+).

Crystallographic analysis of $(\mu\text{-}H)Ru_3(\mu_3\text{-}\eta^3\text{-}CHCHCMe)(CO)_9$ (2)

An orange crystal of **2** was mounted on a glass fiber, which was placed in the beam of a Rigaku AFC-6R diffractometer. Crystal data are given in Table 1. The space group assignment was based on systematic absences of: 0*kl*: $k = 2n$; *h*0*l*: $l = 2n$; *hk*0: $h = 2n$. Intensities of three reflections which were measured after every 150 reflections remained constant throughout data collection indicating crystal stability. The data were corrected for absorption, Lorentz and polarization effects. The structure was solved by direct methods [6]. The non-hydrogen atoms were refined anisotropically. Neutral atom scattering factors were taken from Cromer and Waber [7]. Anomalous dispersion effects were included in F_{calc} [8]; the values for $\Delta f'$ and $\Delta f''$ were those of Cromer [9]. All calculations were performed using the TEXSAN crystallographic software package [10].

TABLE 1. Crystal data for (μ-H)Ru_3(μ_3-η^3-CHCHCMe)$(CO)_9$ (2), (μ-H)Ru_3(μ_3-η^3-CHCHCMe)$(CO)_8(PPh_3)$ (3) and (μ-H)Ru_3(μ_3-η^3-CHCHCMe)$(CO)_7(PPh_3)_2$ (4)

	2	**3**	**4**
Formula	$C_{13}H_6O_9Ru_3$	$C_{30}H_{21}O_8PRu_3$	$C_{47}H_{36}O_7P_2Ru_3$
M	609.40	843.67	1076.95
Space group	*Pbca* (No. 61)	$P\bar{1}$ (No. 2)	$P2_12_12_1$ (No. 19)
a (Å)	15.086(6)	8.840(3)[c]	14.079(3)
b (Å)	18.130(6)	11.046(3)[c]	14.891(3)
c (Å)	12.671(4)	16.607(3)[c]	20.708(3)
Z	8	2	4
V ($Å^3$)	3466(2)	1515(1)	4341(2)
D_{calc} (g cm^{-3})	2.336	1.849	1.649
λ(Mo Kα) (Å)	0.71069	0.71069	0.71069
μ (cm^{-1})	25.75	15.5	11.3
Temperature (°C)	23 ± 1	22 ± 1	22 ± 1
Scan width (°)	1.52 + 0.3 tan θ	0.8 + 0.35 tan θ	0.8 + 0.35 tan θ
Scan type	ω–2θ	θ–2θ	θ–2θ
θ Range (°)	0–50.1	4.0–54.0	4.0–50.0
Total no. reflections measured	3461	6158	8291
No. observed reflections	2303 (3σ)	5373 (3σ)	3884 (3σ)
No. variables	226	382	532
Reflections/parameter ratio	10.19	14.17	7.30
R	0.040[a]	0.026[a]	0.020[a]
R_w	0.048[b]	0.038[b]	0.027[b]

[a] $R = \Sigma||F_o| - |F_c||/\Sigma|F_o|$. [b] $R_w = [\Sigma w(|F_o| - |F_c|)^2/\Sigma w|F_o|^2]^{1/2}$; $w = 1/\sigma^2(|F_o|)$. [c] $\alpha = 108.55(1)$, $\beta = 98.46(2)$, $\gamma = 91.66(2)°$.

Crystallographic analysis of (μ-H)Ru_3(μ_3-η^3-CHCHCMe)$(CO)_8(PPh_3)$ (3)

An orange crystal was attached to the tip of a glass fiber. The X-ray diffraction data were collected on an Enraf-Nonius CAD-4 diffractometer, and the cell constants were determined from a list of reflections found by an automated search routine; details appear in Table 1. All data were corrected for absorption and for Lorentz and polarization effects. The crystal belongs to the triclinic system and space group $P\bar{1}$ was indicated initially by intensity statistics [11] and later confirmed by the successful refinement of the structure. The positions of the Ru and P atoms were determined by direct methods; all remaining non-hydrogen atoms were found in one successive difference Fourier map. All non-hydrogen atoms were refined with anisotropic thermal parameters. The hydrogen atoms of the methyl-allyl group were found in a difference Fourier map and placed into the structure. Refinement calculations were performed on a Digital Equipment Corp. Micro VAX II computer using the CAD4-SDP programs [12]. Neutral atom scattering factors and anomalous scattering corrections were taken from refs. 7 and 9, respectively.

Crystallographic analysis of (μ-H)Ru_3(μ_3-η^3-CHCHCMe)$(CO)_7(PPh_3)_2$ (4)

The analysis was similar to that for complex 3; details appear in Table 1.

Positional and thermal parameters for **2**, **3** and **4** are given in Tables 2–5. ORTEP drawings of these clusters are shown in Figs. 1–3.

Results and discussion

Synthesis and structure of (μ-H)Ru_3(μ_3-η^3-CHCHCMe)$(CO)_9$ (2)

In this study, the 1,3-dimetalloallyltri-ruthenium cluster (μ-H)Ru_3(μ_3-η^3-CHCHCMe)$(CO)_9$ (2) was prepared (Scheme 2) from the reactions of $Ru_3(CO)_{12}$ with 1,3-butadiene or *cis*-2-butene or from $H_4Ru_4(CO)_{12}$ with 1,3-butadiene. The IR and ^{1}H NMR spectra of orange air-stable **2** are the same as those reported [4b] for this compound previously. The ^{13}C NMR assignments are made by comparison with assignments of related dimetalloallyl complexes [13]; the assignment of C(3) is not definitive because it occurs in the range of the CO ligands.

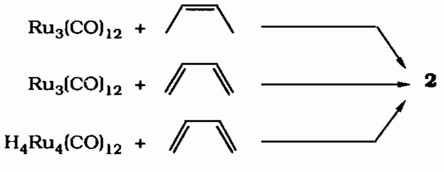

Scheme 2.

The complex ($(\mu\text{-H})Ru_3(\mu_3\text{-}\eta^3\text{-CHCHCMe})(CO)_9$) (2) has a structure (Scheme 1 and Fig. 1) characteristic of related $(\mu\text{-H})Ru_3(\mu_3\text{-}\eta^3\text{-CR}^1\text{CR}^2\text{CR}^3)(CO)_9$ complexes: $(\mu\text{-H})Ru_3(\mu_3\text{-}\eta^3\text{-CMeCHCEt})(CO)_9$ [4c], $(\mu\text{-H})Ru_3(\mu_3\text{-}\eta^3\text{-CMeCMeCMe})(CO)_9$, $(\mu\text{-H})Ru_3(\mu_3\text{-}\eta^3\text{-CMeCMeCOMe})(CO)_9$, $(\mu\text{-H})Ru_3(\mu_3\text{-}\eta^3\text{-CMeCMeCSEt})(CO)_9$ [14] and $(\mu\text{-H})Os_3(\mu_3\text{-}\eta^3\text{-CHCHCOR})(CO)_9$ (R=H or Me) [15], all of which have been studied by X-ray diffraction. They all contain the μ_3-η^3-dimetalloallyl structure with C(1) and C(3) σ bonded to Ru(1) and Ru(3), respectively, and the allyl group π-bonded to Ru(2). Thus, despite the low chemical shift (8.52 ppm) for H(2), the structure of 2 is very similar to those of the other μ_3-η^3-$\text{CR}^1\text{CR}^2\text{CR}^3$ clusters. The equal C(1)–C(2) (1.39(1) Å) and C(2)–C(3) (1.40(1) Å) bond distances are consistent with a delocalized allyl-type ligand. The C(1)–C(2)–C(3) and C(2)–C(3)–C(4) angles are 123.3(7) and 115.4(2)°, respectively.

The Ru(1)–C(1) (2.060(8) Å) and Ru(3)–C(3) (2.095(8) Å) distances are very similar to those in σ-bonded Ru–aryl (2.092 Å) and Ru–vinyl (2.079 Å) complexes [16]. On the other hand, the Ru(2)–C(1) (2.235(7) Å), Ru(2)–C(2) (2.278(8) Å) and Ru(2)–C(3) (2.274(7) Å) distances are significantly longer. As in the previously reported μ_3-η^3-$\text{CR}^1\text{CR}^2\text{CR}^3$ cluster structures, the hydride-bridged Ru(1)–Ru(3) distance (2.941(1) Å) is longer (0.17 Å) than the average of the other two Ru–Ru distances and 0.09 Å longer than the average Ru–Ru distance in $Ru_3(CO)_{12}$ [17]. The C(4) carbon is 0.125 Å out of the C(1)–C(2)–C(3) plane, and H(1) is 0.405 Å out of the Ru(1)–Ru(2)–Ru(3) plane. As noted for other dimetalloallyl complexes [14], the Ru–CO distances (Ru(1)–C(13) and Ru(3)–C(33)) to the CO groups *trans* to C(1) and C(3) of the allyl group are 0.06 Å longer than the average of the other Ru–CO distances.

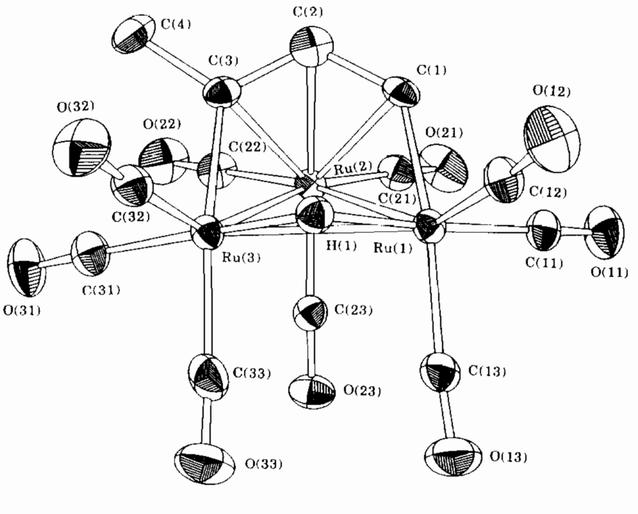

Fig. 1. ORTEP drawing of $(\mu\text{-H})Ru_3(\mu_3\text{-}\eta^3\text{-CHCHCMe})(CO)_9$ (2).

PPh$_3$-substitution products of $(\mu\text{-H})Ru_3(\mu_3\text{-}\eta^3\text{-CHCHCMe})(CO)_9$ (2)

The reaction of 2 with excess or equimolar PPh_3 gives a mixture of the mono- and di-substituted phosphine clusters 3 and 4 in 27 and 15% isolated yields, respectively. Compound *3* was separated as one band by column chromatography; however, ^{1}H NMR analysis shows it to be an approximately 9:1 mixture of two positional isomers. The NMR spectrum of the major isomer is

$$\underset{\textbf{2}}{(\mu\text{-H})Ru_3(\mu_3\text{-}\eta^3\text{-CHCHCMe})(CO)_9} + PPh_3 \longrightarrow$$

$$\underset{\textbf{3}}{(\mu\text{-H})Ru_3(\eta^3\text{-CHCHCMe})(CO)_8(PPh_3)} +$$

$$\underset{\textbf{4}}{(\mu\text{-H})Ru_3(\mu_3\text{-}\eta^3\text{-CHCHCMe})(CO)_7(PPh_3)_2}$$

TABLE 2. Atomic coordinates (×10^4) and B_{eq}[a] for $(\mu\text{-H})Ru_3(\mu_3\text{-}\eta^3\text{-CHCHCMe})(CO)_9$ (2)

Atom	x	y	z	B_{eq} (Å^2)
Ru(1)	8675.4(4)	1877.0(3)	514.7(5)	2.79(3)
Ru(2)	7082.6(4)	1778.2(3)	−586.0(5)	2.70(3)
Ru(3)	7887.9(4)	453.2(3)	−83.4(5)	2.82(3)
O(11)	8854.0(5)	3523(3)	186(6)	6.1(4)
O(12)	9559(5)	1878(4)	2647(6)	6.4(4)
O(13)	10333(5)	1626(4)	−839(6)	6.9(4)
O(21)	6701(6)	3381(3)	−1094(6)	6.7(4)
O(22)	5469(5)	1252(4)	−1811(6)	7.0(4)
O(23)	8434(4)	1580(3)	−2330(5)	4.5(3)
O(31)	6778(5)	−416(4)	−1660(6)	6.3(4)
O(32)	8020(5)	−785(3)	1505(5)	6.0(4)
O(33)	9557(5)	17(4)	−1336(7)	7.3(5)
C(11)	8804(6)	2916(5)	327(7)	4.0(4)
C(12)	9263(6)	1877(4)	1818(7)	3.8(4)
C(13)	9729(6)	1680(5)	−346(7)	4.0(4)
C(21)	6839(6)	2788(5)	−887(7)	4.1(4)
C(22)	6072(6)	1458(5)	−1366(7)	4.0(4)
C(23)	7969(6)	1610(4)	−1606(7)	3.4(4)
C(31)	7189(6)	−102(5)	−1052(8)	4.4(4)
C(32)	7998(6)	−327(5)	891(7)	3.7(4)
C(33)	8959(7)	193(4)	−869(8)	4.5(5)
C(1)	7418(6)	2082(4)	1076(6)	3.1(3)
C(2)	6729(6)	1574(5)	1132(6)	3.5(4)
C(3)	6746(5)	891(4)	618(6)	3.2(3)
C(4)	5901(7)	444(5)	694(8)	5.1(5)
H(1)	8486	940	717	3.3
H(2)	7218	2629	1480	3.7
H(3)	6165	1815	1526	4.2
H(4)	5343	619	1036	6.0
H(5)	6380	449	−8	3.8
H(6)	6041	−91	1209	6.1

[a] $B_{eq} = (8\pi^2/3)\Sigma_{i=1}^{3}\Sigma_{j=1}^{3} U_{ij} a^*_i a^*_j \vec{a}_i \cdot \vec{a}_j$.

reported in 'Experimental'. It has a structure in which the PPh_3 is coordinated at Ru(3) as established by X-ray diffraction studies (see below). In the minor isomer, the PPh_3 is coordinated at Ru(1). The structures of both are readily assigned based on the following NMR data (in $CDCl_3$ solvent): (i) in the methyl region, there is a doublet at 2.18 (d, $J(PH) = 4.45$ Hz) and a singlet at 2.78 in a 9:1 ratio corresponding to the major and minor isomers; (ii) there are two pairs of doublets in the hydride region −19.70 and −19.60 (both have $J(PH) = 15.3$ Hz); (iii) in the ^{13}C NMR spectrum, two signals (37.72 and 38.99 ppm) were observed for the methyl carbon; (iv) two signals (118.01 and 117.60 ppm) were observed for the C(2) carbon; (v) two signals (158.42 and 164.29) for the C(3) carbon were observed; (6) in the ^{31}P NMR spectrum, two signals were observed at 60.26 and 61.49 in a ratio of 9:1.

The structure of the major isomer was unequivocally established by an X-ray diffraction study; an ORTEP plot of **3** is shown in Fig. 2. The basic structure is that of complex **2** (Fig. 1), with the hydride bridging one edge of a triangle of ruthenium atoms. The angle between the planes defined by Ru(1)–Ru(2)–Ru(3) and Ru(1)–C(1)–C(2)–C(3)–Ru(3) is 51.0°. In general, the Ru–Ru distances are longer in **3** than in **2**; thus Ru(1)–Ru(3) is 0.03 Å longer in **3** than **2**, and the average of Ru(1)–Ru(2) and Ru(2)–Ru(3) is 0.01 Å greater in **3** than in **2**. A similar lengthening of Ru–Ru distances is seen [18] in $Ru_3(CO)_{12-x}(L)_x$ clusters as the number of non-carbonyl ligands increases. Thus, the increased electron density made available to the skeleton by replacing CO with PPh_3 results in cluster expansion. The higher electron density on cluster **3** is also indicated by a higher field shift of the methyl protons in **3** (2.18 ppm) as compared with that in **2** (2.82 ppm).

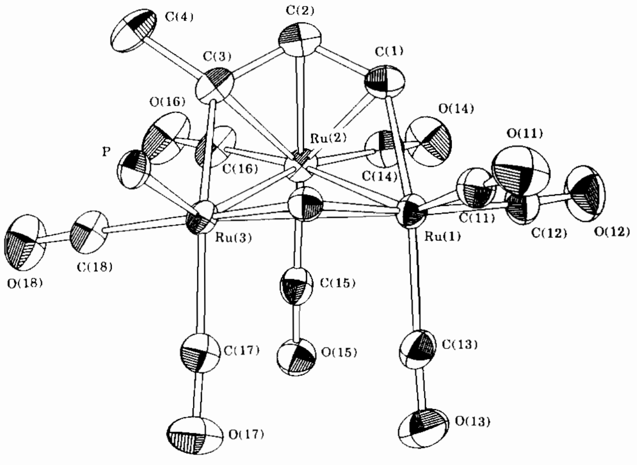

Fig. 2. ORTEP drawing of (μ-H)Ru_3(μ_3-η^3-CHCHCMe)$(CO)_8(PPh_3)$ (**3**). The Ph groups are omitted for clarity.

Elemental analyses for (μ-H)Ru_3(μ_3-η^3-CHCHCMe)$(CO)_7(PPh_3)_2$ (**4**) suggest that the compound results from the substitution of two CO ligands in **2**. But in the ^1H NMR spectrum, signals for H(2) and H(3) were not identified; perhaps they are obscured by the Ph resonances. Clearly H(2) is shifted from its downfield position at 8.52 ppm in **2**. The broadness of the high field hydride signal at −18.5 ppm is presumably caused by coupling to H(3), P(1) and P(2). The methyl

TABLE 3. Positional and thermal parameters and their e.s.d.s for (μ-H)Ru_3(μ_3-η^3-CHCHCMe)$(CO)_8(PPh_3)$ (**3**)

Atom	x	y	z	B (Å^2)[a]
Ru(1)	0.39309(3)	0.20104(2)	0.39955(1)	3.123(5)
Ru(2)	0.52751(3)	0.03259(2)	0.27092(1)	3.303(5)
Ru(3)	0.28661(3)	0.15939(2)	0.21395(1)	2.835(4)
C(1)	0.6039(4)	0.2267(3)	0.3662(2)	3.85(7)
C(2)	0.6323(3)	0.2281(3)	0.2859(2)	3.99(7)
C(3)	0.5176(3)	0.1909(3)	0.2111(2)	3.56(6)
C(4)	0.5785(4)	0.1887(4)	0.1306(2)	5.49(8)
C(11)	0.3582(4)	0.3662(3)	0.4686(2)	4.08(7)
O(11)	0.3383(3)	0.4659(3)	0.5107(2)	6.19(7)
C(12)	0.5027(5)	0.1607(3)	0.4941(2)	4.74(8)
O(12)	0.5731(4)	0.1424(3)	0.5507(2)	7.67(9)
C(13)	0.1993(4)	0.1201(4)	0.4073(2)	4.59(8)
O(13)	0.0905(3)	0.0726(3)	0.4139(2)	7.67(8)
C(14)	0.6679(4)	−0.0396(3)	0.3394(2)	4.83(8)
O(14)	0.7491(4)	−0.0849(3)	0.3777(2)	7.89(9)
C(15)	0.3457(4)	−0.0648(3)	0.2669(2)	4.01(7)
O(15)	0.2482(3)	−0.1368(2)	0.2647(2)	5.06(6)
C(16)	0.5812(5)	−0.0743(3)	0.1659(2)	5.17(8)
O(16)	0.6090(4)	−0.1378(3)	0.1023(2)	7.90(8)
C(17)	0.0841(4)	0.0970(3)	0.2194(2)	3.89(7)
O(17)	−0.0345(3)	0.0540(3)	0.2180(2)	6.09(7)
C(18)	0.2531(4)	0.0593(3)	0.0967(2)	4.33(7)
O(18)	0.2302(4)	−0.0050(3)	0.0262(2)	6.70(8)
P	0.21582(8)	0.34970(6)	0.19454(4)	2.80(1)
C(111)	0.0800(3)	0.3347(3)	0.0973(2)	3.22(6)
C(112)	0.1194(4)	0.2712(3)	0.0170(2)	4.06(7)
C(113)	0.0180(5)	0.2572(4)	−0.0572(2)	5.16(9)
C(114)	−0.1253(5)	0.3027(4)	−0.0532(2)	5.65(9)
C(115)	−0.1658(4)	0.3632(4)	0.0258(2)	5.46(9)
C(116)	−0.0645(4)	0.3794(3)	0.1008(2)	4.17(7)
C(121)	0.3777(3)	0.4555(3)	0.1922(2)	3.15(6)
C(122)	0.3921(4)	0.4962(3)	0.1228(2)	3.99(7)
C(123)	0.5189(4)	0.5757(3)	0.1272(2)	4.97(8)
C(124)	0.6298(4)	0.6151(4)	0.1988(3)	5.37(9)
C(125)	0.6127(4)	0.5763(4)	0.2679(3)	5.25(9)
C(126)	0.4902(4)	0.4972(3)	0.2650(2)	4.28(7)
C(131)	0.1271(3)	0.4583(3)	0.2799(2)	3.16(6)
C(132)	0.1387(4)	0.5885(3)	0.2950(2)	4.84(8)
C(133)	0.0695(5)	0.6704(4)	0.3588(3)	5.8(1)
C(134)	−0.0132(4)	0.6212(4)	0.4062(2)	5.32(9)
C(135)	−0.0306(4)	0.4922(4)	0.3900(2)	4.58(8)
C(136)	0.0403(4)	0.4100(3)	0.3271(2)	3.82(7)

[a] Anisotropically refined atoms are given in the form of the isotropic equivalent displacement parameter defined as: $(4/3)[a^2B(1,1)+b^2B(2,2)+c^2B(3,3)+ab(\cos\gamma)B(1,2)+ac(\cos\beta)B(1,3)+bc(\cos\alpha)B(2,3)]$.

TABLE 4. Positional and thermal parameters and their e.s.d.s for $(\mu\text{-H})Ru_3(\mu_3\text{-}\eta^3\text{-CHCHCMe})(CO)_7(PPh_3)_2$ (**4**)

Atom	x	y	z	B (Å^2)[a]
Ru(1)	0.08478(2)	0.40437(2)	0.51258(1)	2.655(5)
Ru(2)	0.03251(2)	0.36077(2)	0.63971(1)	3.211(5)
Ru(3)	−0.03346(2)	0.52577(2)	0.59481(1)	2.874(5)
C(1)	−0.0143(3)	0.3119(3)	0.5429(2)	3.39(7)
C(2)	−0.0961(3)	0.3268(3)	0.5791(2)	3.67(8)
C(3)	−0.1139(3)	0.4104(3)	0.6102(2)	3.55(7)
C(4)	−0.2007(3)	0.4112(4)	0.6537(2)	4.9(1)
C(5)	0.1808(3)	0.3177(3)	0.5134(2)	3.39(7)
O(5)	0.2382(2)	0.2636(2)	0.5147(2)	5.15(7)
C(6)	0.1737(3)	0.5008(3)	0.5015(2)	4.28(9)
O(6)	0.2264(3)	0.5566(2)	0.4968(2)	7.9(1)
C(7)	0.1045(3)	0.2539(3)	0.6517(2)	4.32(9)
O(7)	0.1510(3)	0.1921(2)	0.6596(2)	6.49(9)
C(8)	−0.0125(4)	0.3581(4)	0.7265(2)	5.5(1)
O(8)	−0.0381(3)	0.3556(4)	0.7780(2)	8.9(1)
C(9)	0.1324(3)	0.4451(3)	0.6480(2)	4.12(8)
O(9)	0.1988(2)	0.4874(2)	0.6612(2)	5.13(7)
C(10)	0.0612(3)	0.6191(3)	0.5910(2)	3.75(8)
O(10)	0.1167(2)	0.6744(2)	0.5936(2)	5.70(8)
C(11)	−0.0607(3)	0.5647(3)	0.6790(2)	4.35(9)
O(11)	−0.0721(3)	0.5850(3)	0.7311(2)	7.02(9)
P(1)	0.06213(6)	0.37554(6)	0.40356(5)	2.88(2)
C(111)	0.1688(3)	0.3623(2)	0.3534(2)	3.27(7)
C(112)	0.1616(4)	0.3206(4)	0.2933(2)	4.67(9)
C(113)	0.2400(4)	0.3128(4)	0.2537(2)	5.4(1)
C(114)	0.3262(3)	0.3469(3)	0.2720(2)	5.3(1)
C(115)	0.3344(3)	0.3877(3)	0.3311(3)	5.1(1)
C(116)	0.2563(3)	0.3960(3)	0.3713(2)	4.11(8)
C(121)	−0.0086(3)	0.4558(3)	0.3575(2)	3.77(8)
C(122)	−0.1013(3)	0.4739(3)	0.3778(2)	4.70(9)
C(123)	−0.1569(4)	0.5332(4)	0.3436(3)	6.3(1)
C(124)	−0.1231(4)	0.5752(4)	0.2904(3)	6.3(1)
C(125)	−0.0335(4)	0.5605(4)	0.2720(3)	7.0(1)
C(126)	0.0241(4)	0.5008(4)	0.3040(2)	5.5(1)
C(131)	0.0055(3)	0.2655(3)	0.3911(2)	3.30(7)
C(132)	0.0570(3)	0.1899(3)	0.4055(2)	4.58(9)
C(133)	0.0161(4)	0.1045(3)	0.4022(2)	5.3(1)
C(134)	−0.0775(4)	0.0970(3)	0.3852(3)	5.4(1)
C(135)	−0.1288(3)	0.1707(4)	0.3698(3)	5.6(1)
C(136)	−0.0890(3)	0.2564(3)	0.3723(2)	4.47(9)
P(2)	−0.14615(7)	0.62020(6)	0.54929(5)	3.17(2)
C(211)	−0.2563(3)	0.5738(3)	0.5152(2)	3.60(7)
C(212)	−0.3336(3)	0.6284(4)	0.5029(3)	6.0(1)
C(213)	−0.4114(4)	0.5982(4)	0.4711(4)	7.5(1)
C(214)	−0.4141(4)	0.5089(4)	0.4501(3)	6.7(1)
C(215)	−0.3415(4)	0.4537(3)	0.4645(3)	5.6(1)
C(216)	−0.2611(3)	0.4851(3)	0.4975(2)	4.09(8)
C(221)	−0.1045(3)	0.6906(3)	0.4828(2)	3.53(7)
C(222)	−0.1552(4)	0.7663(3)	0.4623(3)	5.1(1)
C(223)	−0.1232(4)	0.8166(3)	0.4108(3)	6.1(1)
C(224)	−0.0385(4)	0.7940(4)	0.3806(3)	5.8(1)
C(225)	0.0103(3)	0.7202(3)	0.3999(3)	5.3(1)
C(226)	−0.0203(3)	0.6691(3)	0.4511(2)	4.35(9)
C(231)	−0.1919(3)	0.6996(3)	0.6086(2)	4.01(8)
C(232)	−0.2600(3)	0.6727(4)	0.6523(2)	5.4(1)
C(233)	−0.2914(4)	0.7303(5)	0.7010(3)	7.4(1)
C(234)	−0.2545(5)	0.8131(4)	0.7067(3)	8.3(1)
C(235)	−0.1875(5)	0.8424(4)	0.6656(3)	7.7(1)
C(236)	−0.1546(4)	0.7857(4)	0.6161(3)	6.0(1)

[a] See footnote a in Table 3.

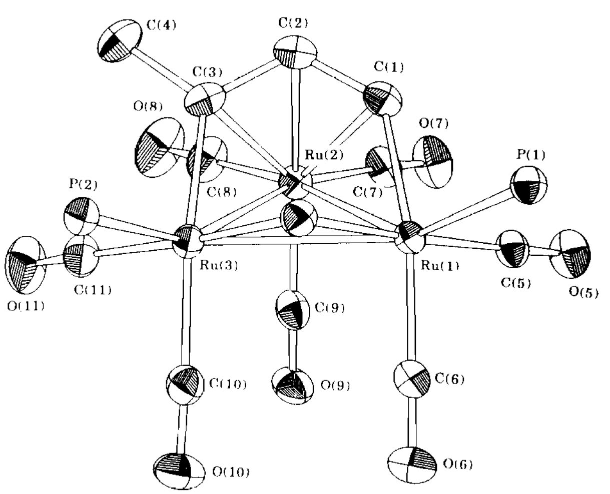

Fig. 3. ORTEP drawing of $(\mu\text{-H})Ru_3(\mu_3\text{-}\eta^3\text{-CHCHCMe})(CO)_7(PPh_3)_2$ (**4**). The Ph groups are omitted for clarity.

protons occur as a doublet at 2.13 (J(HP) = 4.49 Hz). In the ^{13}C NMR spectrum, signals for C(2) and C(3) could be assigned, but none for C(1) was detected; it may have been obscured by the PPh_3 carbons.

Despite uncertainties in the NMR characterization of **4**, the structure of this compound as determined by X-ray diffraction (Fig. 3) shows that it has the same $\mu_3\text{-}\eta^3$-CHCHCMe structure as **2** and **3**, except that there are PPh_3 groups at both Ru(1) and Ru(3). As found in the comparison of **2** and **3**, the additional PPh_3 ligand lengthens the Ru–Ru distances still further. The Ru–H bonds become longer with the added PPh_3; the hydride is 0.4–0.6 Å above the Ru(1)–Ru(2)–Ru(3) plane toward the allyl group in all three of the complexes. The geometry of the allyl ligand remains essentially the same in all of the complexes.

Conclusions

A significant conclusion from these studies is that the $\mu_3\text{-}\eta^3$-CHCHCMe dimetalloallyl group is remarkably stable. It forms in reactions of $Ru_3(CO)_{12}$ with either 1,3-butadiene or *cis*-2-butene. It resists rearrangement or displacement in reactions of $(\mu\text{-H})Ru_3(\mu_3\text{-}\eta^3\text{-CHCHCMe})(CO)_9$ (**2**) with PPh_3, the CO groups being preferentially substituted. Thus, it seems that dimetalloallyl groups would be stable on triangular arrays of atoms on metal surfaces. Yet to our knowledge, such a unit has not been proposed to form on such surfaces. For the system involving ethylene adsorption on Ru/SiO_2 [1], physisorbed *cis*- and *trans*-2-butene and butane are formed; in addition, a chemisorbed species with a ^{13}C NMR signal at 85 ppm is detected. In view of the stability of the $\mu_3\text{-}\eta^3$-dimetalloallyl group in Ru_3 clusters, one might consider this as a possible chem-

TABLE 5. Selected bond distances and angles in $(\mu\text{-H})\text{Ru}_3(\mu_3\text{-}\eta^3\text{-CHCHCMe})(\text{CO})_9$ (**2**), $(\mu\text{-H})\text{Ru}_3(\mu_3\text{-}\eta^3\text{-CHCHCMe})(\text{CO})_8(\text{PPh}_3)$ (**3**) and $(\mu\text{-H})\text{Ru}_3(\mu_3\text{-}\eta^3\text{-CHCHCMe})(\text{CO})_7(\text{PPh}_3)_2$ (**4**)

	2	**3**	**4**
Ru(1)–Ru(2)	2.784(1)	2.7905(3)	2.8096(5)
Ru(2)–Ru(3)	2.766(1)	2.7946(3)	2.7865(5)
Ru(1)–Ru(3)	2.941(1)	2.9690(3)	2.9895(5)
Ru(1)–C(1)	2.060(8)	2.056(3)	2.059(5)
Ru(2)–C(1)	2.235(7)	2.235(3)	2.231(5)
Ru(2)–C(2)	2.278(8)	2.249(3)	2.269(5)
Ru(2)–C(3)	2.274(7)	2.267(3)	2.278(5)
Ru(3)–C(3)	2.095(8)	2.070(3)	2.094(5)
C(1)–C(2)	1.39(1)	1.397(5)	1.398(7)
C(2)–C(3)	1.40(1)	1.422(5)	1.423(8)
C(3)–C(4)	1.51(1)	1.506(5)	1.513(7)
Ru(1)–H(1)	1.742	1.80(4)	1.8198(3)
Ru(3)–H(1)	1.619	1.72(4)	1.8057(4)
Ru(1)–Ru(2)–Ru(3)	63.99(3)	64.23(1)	64.58(1)
Ru(2)–Ru(3)–Ru(1)	58.29(3)	57.82(1)	58.08(1)
Ru(2)–Ru(1)–Ru(3)	57.71(2)	57.95(1)	57.34(1)
Ru(1)–Ru(3)–C(3)	83.7(2)	84.02(9)	83.76(15)
Ru(3)–Ru(1)–C(1)	82.8(2)	82.22(9)	81.6(1)
C(1)–C(2)–C(3)	123.3(7)	122.8(3)	121.5(5)
Ru(3)–C(3)–C(2)	123.2(6)	123.4(2)	123.8(4)
Ru(3)–C(3)–C(4)	121.1(6)	123.1(3)	121.1(4)
Ru(1)–C(1)–C(2)	126.0(6)	126.7(3)	128.5(4)
C(2)–C(3)–C(4)	115.4(7)	113.3(3)	115.0(5)
Ru(1)–H(1)–Ru(3)	122.06	115.36(2)	111.09(2)

isorbed species on the ruthenium metal. This appears not be the case, since the ^{13}C NMR ranges of C(1) (158–159 ppm), C(2) (117–119 ppm) and C(3) (190–195 ppm) in complexes **2**, **3** and **4** are quite different from the 85 ppm signal of the new species on the ruthenium surface.

Supplementary material

Listings of bond distances and angles, thermal parameters and structure factors are available from R.J.A.

Acknowledgements

We thank Professor T. S. King for helpful discussions and Johnson Matthey, Inc. for a loan of RuCl_3. Ames Laboratory is operated for the U.S. Department of Energy by Iowa State University under contract no. W-7405-Eng-82. This research was supported by the Office of Basic Energy Sciences, Chemical Sciences Division and by the Research and Development Exploratory Fund of the Ames Laboratory.

References

1 (a) M. Pruski, J. C. Kelzenberg, B. C. Gerstein and T. S. King, *J. Am. Chem. Soc., 112* (1990) 4232; 9b) M. Sprock, M. Pruski, B. C. Gerstein and T. S. King, *Catal. Lett., 5* (1990) 395; (c) S.-J. Hwang, T. S. King and B. C. Gerstein, *Catal. Lett., 8* (1991) 367.

2 J. E. Evans and G. S. McNulty, *J. Chem. Soc., Dalton Trans.,* (1981) 2017.

3 L. R. Beanan and J. B. Keister, *Organometallics, 4* (1985) 1713.

4 (a) M. Castiglioni, L. Milone, D. Osella, G. A. Vaglio and M. Valle, *Inorg. Chem., 15* (1976) 394; (b) O. Gambino, M. Valle, S. Aime and G. A. Vaglio, *Inorg. Chim. Acta., 8* (1974) 71; (c) M. Evans, M. Hursthouse, E. W. Randall, E. J. Rosenberg, L. Milone and M. Valle, *J. Chem. Soc., Chem. Commun.,* (1972) 545; (d) M. I. Bruce, M. A. Cairns and M. Green, *J. Chem. Soc., Dalton Trans.,* (1972) 1293; (e) S. Aime, G. Jannon, D. Osella and A. J. Deeming, *J. Organomet. Chem., 214* (1981) C15; (f) S. Aime, G. Jannon, D. Osella, J. A. Arce and A. J. Deeming, *J. Chem. Soc., Dalton Trans.,* (1984) 1987; (g) S. Aime, L. Milone, D. Osella and M. Valle, *J. Chem. Res. M, 782* (1978) 77(s); (h) A. P. Humphries and S. A. R. Knox, *J. Chem. Soc., Dalton Trans.,* (1975) 1710; (i) J. W. Ziller, K. D. Bower, M. D. Dennis, J. B. Keister and M. R. Churchill, *Organometallics, 8* (1989) 492; (j) L. R. Beanan, Z. A. Rahman and J. B. Keister, *Organometallics, 2* (1983) 1062.

5 H. D. Kaesz, S. A. R. Knox, J. W. Koepke and R. B. Saillant, *J. Chem. Soc., Dalton Trans.,* (1971) 477.

6 J. C. Calbrese, PHASE – Patterson Heavy Atom Solution Extractor, *Ph.D Thesis,* University of Wisconsin-Madison, 1972; P. T. Beurskens, DIRDIF: Direct Methods for Difference Structures – an automatic procedure for phase extension and refinement of difference structure factors, *Tech. Rep. 1984/1,* Crystallography Laboratory, Toernooiveld, 6525 Ed Nijmegen, Netherlands, 1984.

7 D. T. Cromer and J. T. Waber, in J. A. Ibers and W. C. Hamilton (eds.), *International Tables for X-ray Crystallography,* Vol. IV, Kynoch, Birmingham, UK, 1974, Table 2.2B, p. 99.

8 J. A. Ibers and W. C. Hamilton, *Acta Crystallogr., 17* (1964) 781.

9 D. T. Cromer, in J. A. Ibers and W. C. Hamilton (eds.), *International Tables for X-ray Crystallography,* Vol. IV, Kynoch, Birmingham, UK, 1974, Table 2.3.1, p. 149.

10 TEXSAN: Single Crystal Structure Analysis Software, version 5.0 (1989), Molecular Structure Corporation, The Woodlands, TX 77381, 1989.

11 G. M. Sheldrick, *SHELXS-86,* Institut für Anorganische Chemie der Universität, Göttingen, FRG.

12 *Enraf-Nonius Structure Determination Package,* Enraf-Nonius, Delft, Netherlands.

13 S. Aime, L. Milone, D. Osella, M. Valle and E. W. Randall, *Inorg. Chim. Acta, 20* (1976) 217.

14 M. R. Churchill, L. A. Buttrey, J. B. Keister, W. J. Ziller, T. S. Janik and W. S. Striejewske, *Organometallics, 9* (1990) 766, and refs. therein.

15 B. E. Hanson, B. F. G. Johnson, J. Lewis and P. R. Raithby, *J. Chem. Soc., Dalton Trans.,* (1980) 1852.

16 A. G. Orpen, L. Brammer, F. H. Allen, O. Kennard, D. G. Watson and R. Taylor, *J. Chem. Soc., Dalton Trans. Supl.,* (1989) S1-S83.

17 M. R. Churchill, F. J. Hollander and J. P. Hutchinson, *Inorg. Chem., 16* (1977) 2655.

18 M. I. Bruce, M. J. Liddell, O. B. Shawkataly, I. Bytheway, B. W. Skelton and A. H. White, *J. Organomet. Chem., 369* (1989) 217.